Modal Identification and Environmental Effects on Natural Frequencies Using openLAB Research Bridge

Ronit Baishya * [1]

[1] Department of Civil and Environmental Engineering, Lehigh University, Bethlehem, Pennsylvania, USA

Abstract

Modal-based structural health monitoring only works if you can tell environmental effects apart from real structural change. This study looks at how air temperature and solar radiation shift the natural frequencies of the openLAB Research Bridge, a three-span prestressed concrete structure fitted with accelerometers and environmental sensors.

We paired triggered acceleration records from the bridge's undamaged reference state with concurrent temperature and solar-radiation readings, then ran modal identification to get the dominant frequencies and mode shapes. These were sorted into environmental cases by high and low temperature and solar radiation.

Four frequency clusters emerged, near 4.6, 7.0, 8.5–9.0, and 10.6 Hz, and each shifted depending on the case. Temperature drove more of the variation than solar radiation did. The two also interact: solar radiation matters more when temperatures are low, and temperature matters more when solar radiation is low. These shifts can look like structural deterioration if you're not accounting for them. Any damage indicator built on modal frequencies has to account for the environmental state at the time of measurement, or it risks flagging noise as damage.

Keywords: Structural Health Monitoring; Modal Identification; Environmental Effects

1 Introduction and Background

Vibration-based structural health monitoring (SHM) tracks a structure's condition by repeatedly measuring its dynamic response. Natural frequencies and mode shapes are among the quantities most often pulled from these measurements, since they depend on the mass and stiffness distribution of the structure and can be identified from ambient or triggered vibration without taking the bridge out of service. A shift in either quantity can signal that something in the structure has changed, which is why modal properties are used as damage indicators [8, 10].

Damage isn't the only thing that changes modal properties, though. A bridge measured under different environmental conditions can return different natural frequencies with no structural deterioration at all. Unless the normal environmental variability is characterized first, these shifts can be mistaken for damage

*Correspondence: rrb225@lehigh.edu

[3, 7]. Any scheme that compares a new measurement against a historical value inherits an environmental problem before it inherits a structural one — a damage threshold isn't reliable until the environmental contribution is understood.

Temperature and solar radiation affect a bridge through related but distinct mechanisms. Air temperature can alter the effective elastic properties of concrete and the behavior of bearings and supports. Solar radiation heats the structure unevenly: the deck surface and sun-facing regions warm faster than shaded or lower surfaces, producing thermal gradients that a single air-temperature reading won't capture [3]. These gradients can change the internal stress state, and they don't necessarily affect every vibration mode the same way.

The openLAB Research Bridge works well for studying this because it was built as a large-scale experimental platform for bridge monitoring and digital-twin research [9, 11]. Its monitoring program includes a reference period before planned damaging tests, so the undamaged structure's normal response can be studied across changing environmental and operational conditions. The openLAB dataset provides synchronized structural-response and environmental measurements for exactly this purpose [2].

Other recent SHM work has focused on telling real structural change apart from data anomalies and sensor faults, using statistical, machine-learning, and signal-processing methods for faulty-data detection, anomaly detection, and sensor-fault classification [1, 4–6]. That work points to the same conclusion: you need a reliable description of normal bridge behavior before you can call anything damage.

This study quantifies how air temperature and solar radiation affect the dominant natural frequencies of the openLAB Research Bridge during its undamaged reference condition. We pair triggered acceleration records with concurrent environmental measurements, identify dominant modal frequencies and mode shapes, and compare results across environmental conditions, focusing on the frequency regions near 4.6, 7.0, 8.5–9.0, and 10.6 Hz.

2 Dataset

2.1 The Bridge

The openLAB Research Bridge is a full-scale prestressed concrete bridge built as an experimental platform for structural health monitoring research. It has three spans of roughly 15 m each, for a total length of 45 m, and is about 4.5 m wide [2, 11].

Unlike a conventional in-service monitoring site, this bridge has controlled damage scenarios built into the research program: loading selected girders to their Ultimate Limit State, intentionally damaging individual tendons, and running static and dynamic tests around the coupling joint and critical shear regions.

Before any of that damaging testing happens, a reference monitoring period captures how the undamaged bridge behaves under changing environmental and operational conditions. That baseline matters because it's the only way to tell later, once damage is introduced, whether a change in modal properties actually reflects damage or just normal variability.

2.2 Sensor Layout

An electrical SHM system is installed primarily on Spans 1 and 2, with vibration, deformation, and environmental sensors.

Accelerometers sit at the midspan of the instrumented spans, one per girder, giving vertical acceleration readings at multiple points across the deck. That spatial spread is what makes it possible to identify both natural frequencies and their corresponding mode shapes.

Tiltmeters are installed about 4 m from Axis 20. Per the dataset documentation, this is close to the point of zero bending moment under self-weight, where tilt response should be relatively large.

Environmental sensors mounted above the bridge near Axis 10 record air temperature, humidity, and solar radiation [2]. This study uses the accelerometer data for modal identification and the environmental data to look at how air temperature and solar radiation affect it.

2.3 Dataset

The openLAB dataset contains measurements of acceleration, tilt, air temperature, humidity, and solar radiation. Most environmental measurements are recorded at 10-minute intervals, while triggered acceleration records are acquired during non-damaging load tests and whenever vibration levels increase because of traffic or nearby construction activities [2].

The acceleration data used in this study are obtained from the `01_acceleration_trigger` dataset and cover the undamaged bridge from 1 May to 31 October 2024. Each triggered record contains approximately 70 s of response sampled at 500 Hz.

Triggering occurs when the measured vibration amplitude exceeds approximately

$$2 \times 10^{-4}\,\mathrm{m/s^2}.$$

This approach was adopted because continuously recorded ambient samples frequently contained insufficient vibration energy for reliable modal identification.

Environmental measurements are obtained from the `02_environment` dataset, which contains air temperature, humidity, and solar-radiation data from 1 February to 31 October 2024 at one sample every 10 minutes, corresponding to a sampling rate of approximately

$$\frac{1}{600}\ \mathrm{Hz}.$$

Each acceleration record is associated with its date and time, and the corresponding environmental values are obtained from the environmental time series. When no environmental reading occurs at the exact trigger time, the corresponding value is estimated by linear interpolation between adjacent environmental samples.

3 Methodology

The analysis was designed to pair each triggered acceleration record with the environmental conditions at the time of acquisition, identify the natural frequencies of the bridge from that record, and compare the resulting modal parameters across environmental conditions.

First, the date and time associated with each triggered acceleration file were extracted from the file information. These timestamps were used to obtain the corresponding air-temperature and solar-radiation values from the monthly environmental dataset.

Because environmental measurements were recorded at a coarser interval than the acceleration triggers, values at the trigger times were obtained by interpolation when an exact environmental sample was unavailable.

Modal identification was then performed from the acceleration measurements. The frequency-domain response was examined for dominant peaks, and the corresponding natural frequencies and mode shapes were identified.

Four frequency regions were consistently observed in the analyzed records:

- approximately 4.6 Hz,
- approximately 7.0 Hz,
- approximately 8.5–9.0 Hz, and
- approximately 10.6 Hz.

The analysis was therefore concentrated on these frequency regions.

The records were next grouped according to air temperature and solar radiation. Air temperature was divided at 18°C and solar radiation at $80\,\mathrm{W/m^2}$.

The environmental grouping is summarized in Table 1.

Table 1: Environmental grouping of the triggered acceleration records.

	$T < 18°\mathrm{C}$	$T \geq 18°\mathrm{C}$
$S \geq 80\,\mathrm{W/m^2}$	Group 2	Group 1
$S < 80\,\mathrm{W/m^2}$	Group 4	Group 3

Within each environmental condition, the natural frequencies of the selected acceleration records were computed and averaged to obtain representative values for each modal region.

Pairwise differences between representative values were then used to examine the influence of solar radiation and air temperature while the other environmental variable was held approximately fixed.

The source analysis also reports a fifth case in the modal-result tables. Because the underlying source does not define this fifth case within the four-group 2×2 classification above, Case V is retained in the results exactly as reported rather than reassigned to one of Groups 1–4.

4 Results and Discussion

Modal identification returned four consistent frequency regions across the triggered records, near 4.6, 7.0, 8.5–9.0, and 10.6 Hz. Each region is examined below against the environmental conditions recorded at the time of measurement.

4.1 Environmental Variation

Figure 1 shows the variation of air temperature and solar radiation over the monitoring period. Both parameters vary considerably, providing records over a broad range of environmental conditions.

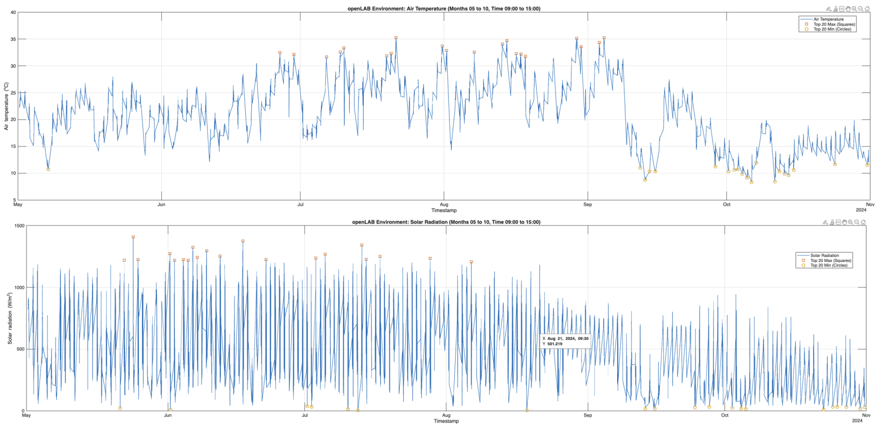

Fig. 1: Air temperature and solar radiation over the monitoring period.

4.2 Modal Frequency near 4.6 Hz

Table 2 summarizes the frequencies identified near 4.6 Hz. The means for Cases I–IV fall within a relatively narrow range of 4.56–4.68 Hz.

Case V gives a higher mean of 4.96 Hz, influenced by two records at 5.19 and 5.26 Hz that lie above the remaining measurements in this modal region.

Table 2: Identified natural frequencies near 4.6 Hz.

Case	File 1	File 2	File 3	File 4	File 5	Mean
I	4.67	4.81	4.61	4.67	4.63	**4.68**
II	–	4.68	–	–	–	**4.68**
III	4.64	–	4.57	4.43	4.60	**4.56**
IV	4.53	–	4.54	4.59	4.63	**4.57**
V	–	–	4.42	5.19	5.26	**4.96**

The corresponding mode-shape result for this frequency region is shown in Fig. 2.

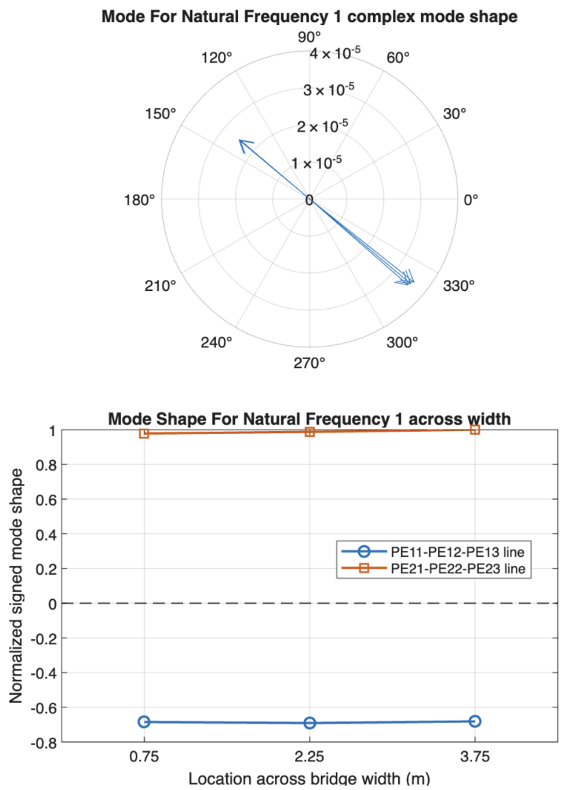

Fig. 2: Mode shape for the 4.6 Hz region.

4.3 Modal Frequency near 7 Hz

Cases I, III, and IV agree within approximately 0.01 Hz in the second modal region, with mean frequencies of 6.98–6.99 Hz. This mode is therefore the least sensitive of the four principal frequency regions to the environmental state represented by these cases.

Case V gives a higher mean of 7.21 Hz. No peak was identified in this region for Case II.

Table 3: Identified natural frequencies near 7 Hz.

Case	File 1	File 2	File 3	File 4	File 5	Mean
I	–	–	–	6.98	–	**6.98**
II	–	–	–	–	–	–
III	–	–	7.02	6.94	–	**6.98**
IV	7.00	6.99	–	7.02	6.94	**6.99**
V	–	–	7.04	–	7.37	**7.21**

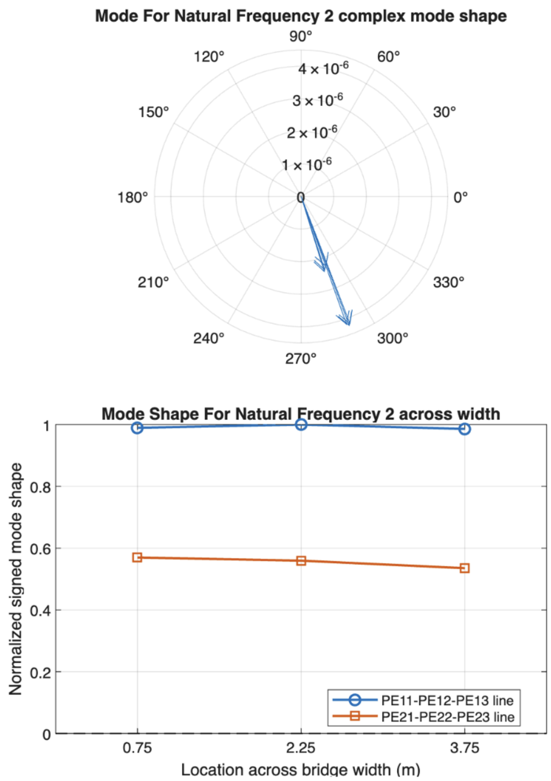

Fig. 3: Mode shape for the 7 Hz region.

4.4 Modal Frequency near 8.5–9 Hz

The third modal region shows the widest spread of the four, from 8.07 to 8.98 Hz in the reported case means.

The low value comes from Case III, where the mode was identified in only one selected record. The remaining identified individual values in Table 4 fall between 8.66 and 9.11 Hz.

Consequently, the apparent spread in this region should be interpreted cautiously because part of it rests on a single measurement.

Table 4: Identified natural frequencies near 8.77 Hz.

Case	File 1	File 2	File 3	File 4	File 5	Mean
I	–	9.05	8.73	–	8.77	**8.85**
II	–	8.74	9.11	9.08	–	**8.98**
III	8.07	–	–	–	–	**8.07**
IV	–	8.66	–	8.73	–	**8.70**
V	–	–	–	–	–	–

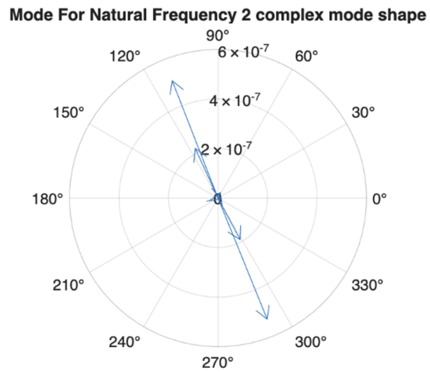

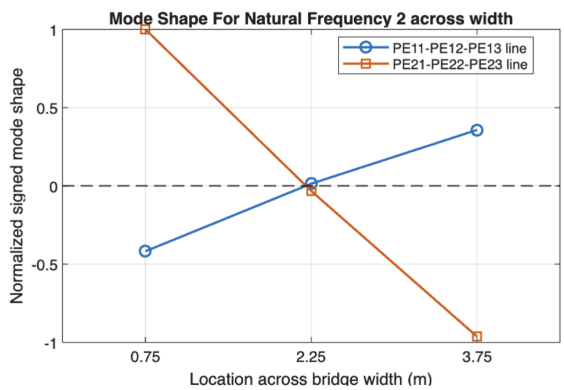

Fig. 4: Mode shape for the 8.77 Hz region.

4.5 Modal Frequency near 10.6 Hz

The fourth modal region is identified around 10.6 Hz. Mean frequencies range from 10.40 Hz in Case V to 10.89 Hz in Case II.

Case V includes one value at 9.80 Hz, which is substantially below the other values in that row and contributes to the lower case mean.

Table 5: Identified natural frequencies near 10.60 Hz.

Case	File 1	File 2	File 3	File 4	File 5	Mean
I	10.61	10.87	–	–	–	**10.74**
II	10.88	–	–	10.95	10.83	**10.89**
III	–	10.68	10.57	10.36	10.50	**10.53**
IV	10.59	–	–	10.59	10.68	**10.62**
V	10.50	10.93	10.58	9.80	10.21	**10.40**

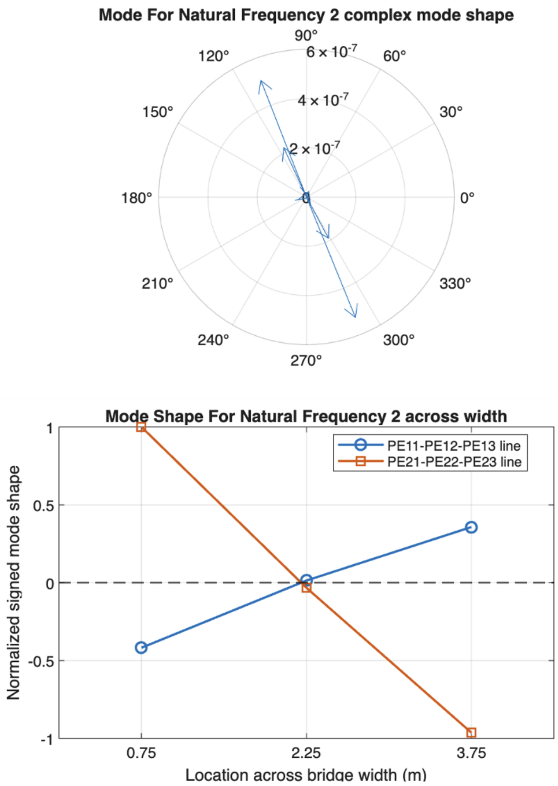

Fig. 5: Mode shape for the 10.60 Hz region.

4.6 Comparison Across Modes

Table 6 combines the mean values for the four modal regions.

The modes do not respond equally to environmental variation. The approximately 7 Hz mode remains comparatively stable across Cases I, III, and IV, while the 8.5–9 Hz region exhibits the greatest reported variation.

The 4.6 and 10.6 Hz modes show intermediate levels of variability.

Table 6: Mean natural frequencies (Hz) by environmental case.

Case	4.6 Hz	7.0 Hz	8.5–9 Hz	10.6 Hz
I	4.68	6.98	8.85	10.74
II	4.68	–	8.98	10.89
III	4.56	6.98	8.07	10.53
IV	4.57	6.99	8.70	10.62
V	4.96	7.21	–	10.40

4.7 Separating Solar Radiation from Air Temperature

Pairwise comparisons were used to investigate changes in one environmental variable while the other was held approximately fixed.

The reported frequency changes are summarized in Table 7.

Table 7: Frequency change (Hz) with each environmental variable, holding the other approximately fixed.

Variable	Cases (condition held)	4.6 Hz	7.0 Hz	8.5–9 Hz	10.6 Hz
Solar radiation	I–IV (high T)	0.11	-0.01	0.15	0.12
Solar radiation	III–V (low T)	-0.40	-0.23	–	0.12
Air temperature	I–III (high S)	0.12	0.00	0.78	0.21
Air temperature	IV–V (low S)	-0.38	-0.22	–	0.22

At high temperature, changing solar radiation shifts the reported modal frequencies by approximately -0.01 to 0.15 Hz.

Under low-temperature conditions, larger changes appear in the lower modes, including -0.40 Hz and -0.23 Hz. The results therefore indicate that the influence of solar radiation is more pronounced when the bridge is colder.

Temperature shows a comparable interaction with solar radiation. Under high solar radiation, the reported modal-frequency changes are 0.12, 0.00, 0.78, and 0.21 Hz.

Under low solar radiation, the available modes change by -0.38, -0.22, and 0.22 Hz.

The 0.78 Hz value in the 8.5–9 Hz region is the largest reported change, although it depends on the single Case III record noted above.

Taken together, the results indicate that air temperature changes the identified frequencies more strongly than solar radiation in the analyzed sample.

Neither effect appears independent of the other: solar radiation has a larger influence at lower temperatures, while temperature has a larger influence when solar radiation is low.

All records considered in this analysis correspond to the undamaged bridge. Therefore, shifts of comparable magnitude in future monitoring data cannot automatically be interpreted as damage without considering the environmental state at the time of measurement.

4.8 Physical Interpretation

Natural frequency is governed by the mass and stiffness distribution of the structure.

For an idealized beam-like system, the dependence may be expressed schematically as

$$f_n \propto \frac{n^2}{2\pi L^2}\sqrt{\frac{EI}{\rho A}}. \tag{1}$$

Here, E is the effective elastic modulus, I is the second moment of area, ρ is density, A is cross-sectional area, and L is a characteristic span length.

Thermal conditions can alter effective stiffness through the temperature dependence of material properties, bearing and support behavior, and thermally induced internal stresses.

Solar radiation can additionally generate vertical and transverse temperature gradients.

These mechanisms provide a physical basis for environmentally induced frequency shifts, but the present analysis does not isolate their individual contributions.

The reported shifts should therefore be interpreted as empirical environmental effects rather than predictions from a validated thermal-structural model.

5 Conclusions

The identified modal frequencies of the openLAB Research Bridge shift with environmental conditions, even though every record analyzed here comes from the undamaged reference state. The four principal modal regions don't respond equally, and air temperature and solar radiation don't act independently of each other.

The 7 Hz mode is the most stable of the four, with mean values of 6.98, 6.98, and 6.99 Hz across Cases I, III, and IV — barely moving. The 8.5–9 Hz region moves the most. The 4.6 and 10.6 Hz regions fall somewhere in between.

That mode-dependent behavior matters for picking damage indicators: a mode that barely reacts to environmental variation makes a more stable reference baseline than one that does.

Pairwise comparisons show solar radiation has a bigger effect at lower air temperatures, and temperature has a bigger effect when solar radiation is low. Overall, temperature drives more of the frequency change in this sample than solar radiation does.

In practical terms, this means shifts of several tenths of a hertz can happen with no damage involved. So any damage-detection strategy built on modal frequencies needs environmental normalization or compensation before it treats a change as structural deterioration.

6 Limitations

The dataset comes with several limitations worth flagging.

Triggered acceleration records only exist when vibration crosses the prescribed threshold, so the sample skews toward higher-excitation events. Coverage across environmental cases is also uneven — some case means rest on just one or two identified records, which makes it hard to tell a real environmental shift from ordinary modal-identification scatter.

There are known data-quality issues too. Some sensors had periods of data loss or abnormal signals, and electrical interference around 50 Hz and its harmonics shows up in the measurements. That interference sits well above the 4–11 Hz band this study focuses on, but sensor faults and anomalous readings are still worth keeping in mind for vibration-based SHM generally [1, 4, 6].

Given the small sample size in some environmental groups, the safer conclusion here is the overall ranking and interaction of environmental effects, not the exact value of any single frequency shift. The large change reported in the 8.5–9 Hz region especially needs caution — one of the case means behind it comes from a single identified record.

7 Future Scope

This study is a first pass at how air temperature and solar radiation influence the modal frequencies of the openLAB Research Bridge in its undamaged state. Several extensions would strengthen it.

The most immediate is more data. Extending the analysis beyond the May–October window to the full reference period would add records to each environmental condition and widen the temperature range covered. It would also clarify whether the reversal seen in the direction of some temperature effects actually holds up, or whether it's just an artifact of limited coverage.

With a larger dataset, the discrete high/low grouping used here could give way to a continuous environmental baseline model. Rather than sorting measurements into bins, regression or other data-driven methods could model the normal relationship between environmental variables and modal parameters directly, and residual deviations from that baseline could serve as candidate anomaly or damage indicators [5, 7]. This would preserve information near the environmental thresholds instead of losing it to arbitrary cutoffs.

It's also worth testing damage-sensitive features besides natural frequencies, which are convenient to extract but not necessarily the most sensitive to local damage. Future work could compare them against other signal-based or modal indicators and see which responds most to structural change versus environmental variability.

Physics-based finite-element modeling is another useful direction. A calibrated model could show how realistic thermal fields alter individual modes and separate temperature-induced stiffness changes from other mechanisms. Once the planned damaging tests happen, measurements from the damaged bridge can then be checked against the environmentally compensated baseline built from the intact structure — combining data-driven monitoring with physics-based interpretation should sharpen both damage detection and severity assessment.

Finally, the monitoring dataset includes humidity and thermal history, neither of which this study uses. A bridge that's stayed warm for several days won't necessarily have the same internal thermal state as one that just reached the same air temperature. Adding humidity, lagged environmental variables, and thermal-history descriptors could improve how well modal properties are normalized for environmental effects.

Data Availability Statement

The data analyzed in this study are publicly available through the openLAB Research Bridge dataset at https://opara.zih.tu-dresden.de/items/6653124a-8659-40b8-817e-51250639c95b.

The dataset contains structural-response and environmental-monitoring data collected from the openLAB Research Bridge and was used for the modal-identification and environmental-effect analyses presented in this study.

Acknowledgments

The author gratefully acknowledges Dr. Kevin Theunissen for his guidance and support throughout this research and Prof. Shamim N. Pakzad for his supervision, mentorship, and valuable feedback during the development of this work.

ChatGPT (OpenAI) was used as a supporting tool to assist with understanding technical concepts and for English-language editing and grammatical corrections.

The author reviewed and verified the final content and takes full responsibility for the accuracy and interpretation of the work.

Conflicts of Interest

The author declares no conflicts of interest.

References

[1] X. Jian, H. Zhong, Y. Xia, and L. Sun, "Faulty data detection and classification for bridge structural health monitoring via statistical and deep-learning approach," *Structural Control and Health Monitoring*, vol. 28, e2824, 2021. https://doi.org/10.1002/stc.2824

[2] A. Jansen, M. Herbers, B. Richter, M. Walker, F. Jesse, and S. Marx, "Monitoring data of the openLAB research bridge – Part 1: Reference condition," *Data in Brief*, vol. 60, 111624, 2025. https://doi.org/10.1016/j.dib.2025.111624

[3] M. van de Velde, D. Anastasopoulos, H. De Backer, E. Reynders, and G. Lombaert, "Modal strain monitoring of a post tensioned concrete girder bridge: Influence of temperature and solar irradiation," *Engineering Structures*, vol. 329, 119832, 2025. https://doi.org/10.1016/j.engstruct.2025.119832

[4] E. Lydakis, H. Koss, R. Brincker, and S. D. R. Amador, "Data-driven sensor fault diagnosis for vibration-based structural health monitoring under ambient excitation," *Measurement*, vol. 237, 115232, 2024. https://doi.org/10.1016/j.measurement.2024.115232

[5] J. N. Abraham, M. Q. Tran, J. S. Jayaraj, J. C. Matos, M. R. Valluzzi, and S. N. Dang, "Unsupervised learning-based anomaly detection for bridge structural health monitoring: Identifying deviations from normal structural behaviour," *Sensors*, vol. 26, 561, 2026. https://doi.org/10.3390/s26020561

[6] J.-H. Bartels, G. Qian, and M. D. Todd, "Matched filtering-based sensor fault classification for structural health monitoring systems," in *Proceedings of the 15th International Workshop on Structural Health Monitoring (IWSHM 2025)*, Stanford, CA, USA, 9–11 September 2025, pp. 306–314. https://doi.org/10.12783/shm2025/37306

[7] M. Zhou and Z. Lai, "Structural damage classification under varying environmental conditions and unknown classes via open set domain adaptation," *Mechanical Systems and Signal Processing*, vol. 218, 111561, 2024. https://doi.org/10.1016/j.ymssp.2024.111561

[8] S. L. Desjardins and D. T. Lau, "Enhanced operational modal analysis and change point detection for vibration-based structural health monitoring of bridges," *Journal of Infrastructure Intelligence and Resilience*, vol. 3, 100121, 2024. https://doi.org/10.1016/j.iintel.2024.100121

[9] M. Herbers, B. Richter, J.-H. Bartels, T. Al-Zuriqat, K. Smarsly, and S. Marx, "openLAB - A large-scale demonstrator for advancing digital twin developments of bridges," in *ReConStruct: Resilient Concrete Structures*, R. S. Henry and A. Palermo, Eds. International Federation for Structural Concrete (fib),2024, pp. 2057–2067.

[10] G. Namjoshi, P. Williams, and T. Matarazzo, "Modal Property Identification of the Bear Mountain Bridge," in *Topics in Modal Analysis & Parameter Identification II, Vol. 10: Proceedings of the 43rd IMAC, A Conference and Exposition on Structural Dynamics 2025*, B. Dilworth, T. Marinone, and J. Furlich, Eds. River Publishers, 2025, pp. 37–42. https://doi.org/10.13052/97887-438-0155-9_6

[11] M. Herbers, J.-H. Bartels, B. Richter, F. Collin, L. Ulbrich, T. Al-Zuriqat, C. Chillón-Geck, H. Naraniecki, O. Hahn, F. Jesse, K. Smarsly, and S. Marx, "openLAB – Eine Forschungsbrücke zur Entwicklung eines digitalen Brückenzwillings," *Beton- und Stahlbetonbau*, vol. 119, pp. 169–180, 2024. https://doi.org/10.1002/best.202300094